

Inference About the Plastic Behavior of Materials from Experimental Data

Kenneth M. Hanson

Los Alamos National Laboratory, MS-D413
Los Alamos, New Mexico 87545, USA
E-mail: kmh@lanl.gov

Abstract: Key to understanding the uncertainties in a physics simulation code is the full characterization of the uncertainties in the physics submodels incorporated in it. I demonstrate an approach to the determining the parameters of material models in a simulation code that combines the principles of physics and probabilistic Bayesian analysis. The focus is on the parameters and their uncertainties in the simulation-code submodels, as well as the numerical errors introduced in solving the dynamical equations. Bayesian analysis provides the underpinning for quantifying the uncertainties in models inferred from experimental results, which possess their own degree of uncertainty. The aim is to construct an uncertainty model for the submodels that is based on inferences drawn from comparing the code's predictions to relevant experimental results. As an example, I will present a preliminary analysis of a set of material-characterization experiments performed on tantalum to determine the parameters of the Preston-Tonks-Wallace model for plastic material behavior. I will indicate how data from a Taylor impact test may be used to update the parameters in the model by using Bayesian calibration in the context of a simulation code.

Keywords: plastic deformation model, Preston-Tonks-Wallace model, uncertainty analysis, Bayesian analysis, hierarchy of experiments, simulation uncertainty, model uncertainty, systematic uncertainty, Hopkinson-bar experiments, quasistatic-compression experiments

1. INTRODUCTION

The primary sources of data that are typically used to characterize the plastic behavior of a metal are obtained in quasi-static and Hopkinson-bar experiments. In quasi-static tests, a small cylinder of the material is typically squeezed at a constant, relatively slow rate and the change in its height is measured as a function of the load on the cylinder. These measurements are easily converted to stress and strain values. In Hopkinson-bar experiments, an elastic wave is transmitted through a thin cylinder of the material and its change in dimensions measured. Although these measurements require the use of a simulation code for precise interpretation, they are straightforwardly converted to a stress-strain curve at nearly constant strain rate. The strain rates attained in Hopkinson-bar experiments are around 10^3 per second, whereas in quasi-static tests they are typically about one per second or less.

Author's web URL: <http://public.lanl.gov/kmh/>

The analysis of these basic data is a fairly straightforward data-fitting problem, albeit a nonlinear one. The approach used here is quite standard. It is based on linearizing the response of the model output with respect to its input. The Jacobian, which characterizes the first-order sensitivities of the model, is used to minimize chi squared, that is, the mean-square differences between model predictions and the measured data, normalized to their variance. The Jacobian is also used to estimate the quadratic behavior of chi squared, and hence, the covariance matrix of the estimated parameters.

In the present example, it is necessary to introduce systematic uncertainties to account for sample-to-sample variations in material properties. The treatment of systematic uncertainties in analyzing experimental data is a topic that has not received enough attention in most analyses, let alone in the literature. The present analysis incorporates the systematic uncertainties in a straightforward way.

A major goal of any analysis is to transcribe uncertainties in the data into uncertainties in the fitted parameters. A useful self-consistency check on the results of the analysis involves propagating the uncertainties in the parameters (by means of a Monte Carlo procedure) to uncertainties in the stress-strain curves given by the PTW model. The uncertainty in the curves can be compared to the original data relative to their uncertainties to demonstrate that the model used in the analysis is consistent with the data. This test amounts to mapping the uncertainties in the data into the parameters and back again. In the context of the proposed framework [1–3], it is possible to design new experiments that can best provide data for reducing prediction uncertainty.

2. LIKELIHOOD ANALYSIS

Before describing the details of the present analysis, I will briefly review a standard approach to fitting a nonlinear model to data by the minimum chi-squared method [4]. It is assumed that one has a model to predict the values of the measured data. For each measured datum d_i , the model provides a value y_i in terms of the operating conditions of the experiment x_i and a parameter vector \mathbf{a} .

The likelihood is the probability of the measured data for a specified parameter vector \mathbf{a} . If the errors in the data are Gaussian distributed and statistically independent, the likelihood is given by

$$p(\mathbf{d} | \mathbf{a}) \propto \exp \left\{ -\frac{1}{2} \sum_i \frac{[d_i - y_i(\mathbf{a})]^2}{\sigma_i^2} \right\} = \exp \left\{ -\frac{1}{2} \chi^2 \right\} , \quad (1)$$

where σ_i is the expected rms deviation of the measurement d_i , The corresponding value given by the model for a specified parameter vector \mathbf{a} is designated by y_i . One recognizes the sum in the exponential in Eq. (1) as the familiar chi squared, χ^2 , which quantifies the discrepancy between measurements and values predicted by a model.

The parameters that best fit the data are typically taken as those that maximize the likelihood, or equivalently, minimize χ^2 . A standard tactic is to expand the model value y_i

around a particular value of the parameter vector \mathbf{a}^0 and at the value of the independent variable x_i in terms of a Taylor series,

$$y_i = y(x_i, \mathbf{a}) = y_i^0 + \sum_j \left. \frac{\partial y_i}{\partial a_j} \right|_{\mathbf{a}^0} (a_j - a_j^0) + \dots, \quad (2)$$

where $y_i^0 = y(x_i, \mathbf{a}^0)$. The complete set of derivatives make up the so-called the Jacobian matrix \mathbf{J} , which summarizes the results of a first-order sensitivity analysis. Dropping higher-order terms, chi-squared can be approximated as a quadratic function around its minimum,

$$\chi^2(\mathbf{a}) = \frac{1}{2}(\mathbf{a} - \hat{\mathbf{a}})^T \mathbf{K}(\mathbf{a} - \hat{\mathbf{a}}) + \chi^2(\hat{\mathbf{a}}), \quad (3)$$

where $\hat{\mathbf{a}}$ is the parameter vector at the minimum in χ^2 , and \mathbf{K} is the curvature matrix of $\chi^2(\mathbf{a})$ at $\hat{\mathbf{a}}$, which is commonly called the Hessian. The curvature can be written in terms of the Jacobian, evaluated at $\hat{\mathbf{a}}$, as

$$[\mathbf{K}]_{jk} = \left. \frac{\partial^2 \chi^2}{\partial a_j \partial a_k} \right|_{\hat{\mathbf{a}}} = \mathbf{J}\mathbf{J}^T, \quad (4)$$

As noted above, when a flat prior is assumed, the posterior is proportional to the likelihood. In the quadratic approximation for χ^2 given in Eq. (3), the posterior is then a Gaussian

$$p(\mathbf{a} | \mathbf{d}) = \frac{1}{\det(\mathbf{C})(2\pi)^{n/2}} \exp \left\{ -\frac{1}{2}(\mathbf{a} - \hat{\mathbf{a}})^T \mathbf{C}^{-1}(\mathbf{a} - \hat{\mathbf{a}}) \right\}, \quad (5)$$

which is written in a way to explicitly display the covariance matrix, \mathbf{C} :

$$\text{cov}(\mathbf{a}) = \langle (\mathbf{a} - \hat{\mathbf{a}})^T (\mathbf{a} - \hat{\mathbf{a}}) \rangle = \mathbf{C} = 2\mathbf{K}^{-1}. \quad (6)$$

The covariance matrix describes the degree of correlation among the uncertainties in the parameters. The analysis of nearly every type of experiment leads to off-diagonal terms in the covariance matrix, which must be stated for a full specification of the uncertainties in the parameters. The off-diagonal elements of the covariance matrix are often expressed in terms of the correlation coefficients, $\rho_{ij} = C_{ij} / \sqrt{C_{ii}C_{jj}}$.

Once the parameters and their uncertainties are obtained for a given set of experimental data, one may check their consistency with the input data by propagating random Monte Carlo draws from the inferred uncertainty distribution in the parameter space back into the data space. To draw random parameters from a Gaussian distribution with a specified covariance, one can employ a standard numerical technique: one draws a vector \mathbf{r} with the same dimension as the parameter vector \mathbf{a} from an uncorrelated unit-variance Gaussian distribution, and then calculates $\mathbf{a}^* = \mathbf{C}^{\frac{1}{2}}\mathbf{r} + \hat{\mathbf{a}}$. Here the matrix $\mathbf{C}^{\frac{1}{2}}$ is the square root of the covariance matrix, which may be calculated through singular-value or Cholesky decomposition [5]. The set of \mathbf{a}^* will have the mean value of $\hat{\mathbf{a}}$ and the covariance \mathbf{C} .

3. MATERIAL-CHARACTERIZATION MODEL

The Preston-Tonks-Wallace (PTW) model [6] describes the plastic deformation of metals in terms of the dependence of plastic stress on plastic strain over a wide range of strain rates and temperature. The following summary of the PTW model is taken directly from Ref. 6.

In the PTW model, the plastic stress in a material is a function of the amount of strain ψ it has undergone, the strain rate $\dot{\psi}$, the material temperature T , and its density ρ . It is assumed that the plastic stress is independent of the history of the material. Furthermore, PTW ignores nonisotropic plasticity and material texture effects. Material fracture or failure is not included in PTW.

The PTW model is written in terms of three scaled dimensionless variables. The scaled stress variable is $\hat{\tau} = \tau/G(\rho, T)$, where τ is the flow stress, which is one-half the usual von Mises equivalent deviatoric stress σ , that is, $\tau = \sigma/2$, and $G(\rho, T)$ is the shear modulus, which is a function of the material density ρ and temperature T . The shear modulus is taken to be $G(\rho, T) = G_0(\rho) (1 - \alpha \hat{T})$, where $G_0(\rho)$ is the shear modulus at $T = 0$ and $\alpha > 0$ is a material parameter. The material temperature is scaled to its melt temperature T_m , which is a function of the material density ρ , $\hat{T} = T/T_m(\rho)$. For plastic flow, clearly $\hat{T} < 1$. The equivalent plastic strain is denoted by ψ . The strain rate $\dot{\psi}$ is scaled to an appropriate rate

$$\dot{\xi}(\rho, T) = \frac{1}{2} \left(\frac{4\pi\rho}{3M} \right)^{\frac{1}{3}} \left(\frac{G}{\rho} \right)^{\frac{1}{2}}, \quad (7)$$

where M is the atomic mass of the metal. $\dot{\xi}$ is the reciprocal of the time for a transverse sound wave to cross an atom. The strain rate always appears in the PTW formulas in terms of the ratio $\dot{\psi}/\dot{\xi}$.

For any fixed values of strain rate and temperature, the scaled stress $\hat{\tau}$ ranges between the lower and upper limits given by the yield stress $\hat{\tau}_y$ and the saturation value $\hat{\tau}_s$. The functional form for $\hat{\tau}$ depends on the strain ψ as follows

$$\hat{\tau} = \hat{\tau}_s + \frac{1}{p} (s_0 - \hat{\tau}_y) \ln \left\{ 1 - [1 - \exp(-pr)] \exp \left[-\frac{p\theta\psi}{(s_0 - \hat{\tau}_y) [\exp(pr) - 1]} \right] \right\}, \quad (8)$$

where p and θ are material-specific parameters and $r = (\hat{\tau}_s - \hat{\tau}_y)/(s_0 - \hat{\tau}_y)$. The parameter s_0 is explained below.

At strain rates below 10^8 s^{-1} for tantalum at room temperature, the plastic deformation process is controlled by thermal activation. The values for $\hat{\tau}_y$ and $\hat{\tau}_s$ are given by

$$\hat{\tau}_y = y_0 - (y_0 - y_\infty) \operatorname{erf} \left[\kappa \hat{T} \ln \left(\frac{\gamma \dot{\xi}}{\dot{\psi}} \right) \right], \quad (9)$$

$$\hat{\tau}_s = s_0 - (s_0 - s_\infty) \operatorname{erf} \left[\kappa \hat{T} \ln \left(\frac{\gamma \dot{\xi}}{\dot{\psi}} \right) \right], \quad (10)$$

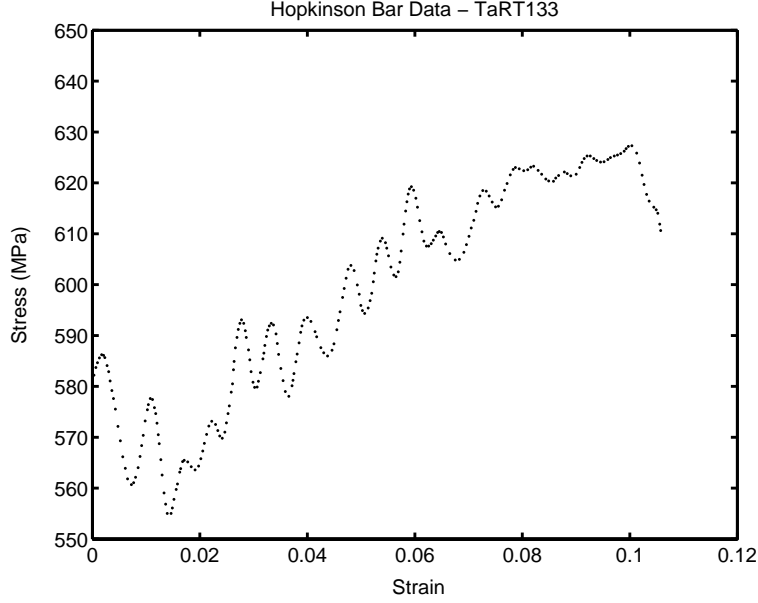


Figure 1. Plot of data obtained from Hopkinson-bar experiment done on tantalum at room temperature and a strain rate of 1300 s^{-1} .

where κ and γ are dimensionless material-related parameters. The error function, defined as $\text{erf}(x) = \frac{2}{\sqrt{\pi}} \int_0^x \exp(-t^2) dt$, has the limiting values $\text{erf}(0) = 0$ and $\text{erf}(\infty) = 1$. Note that the logarithm is nonnegative because $\gamma \dot{\xi} / \dot{\psi} \geq 1$ in the low-strain-rate regime. Therefore, the argument of the error function is nonnegative. The parameters y_0 and y_∞ are the values that $\hat{\tau}_y$ takes at zero temperature and very high temperatures, respectively; s_0 and s_∞ have analogous meanings for $\hat{\tau}_s$.

The PTW model is designed to extend the range of normal plastic-flow models to very high strain rates, above 10^8 s^{-1} , in which regime it relies on Wallace’s theory of overdriven shocks in metals [7]. Because Taylor experiments, which are the goal of the present study, do not reach these very high strain rates, the formulas that apply in that regime will not be given. Suffice it to say that the PTW parameters β , y_1 , and y_2 do not have an effect in the lower strain-rate region.

4. ANALYSIS OF MATERIAL-CHARACTERIZATION EXPERIMENTS

I now outline the analysis of the material-characterization experiments to estimate the PTW parameters and their uncertainty. In a sense, the approach is a straightforward chi-squared (or least-squares) analysis, but it has some noteworthy aspects, for example, the inclusion of systematic uncertainties.

Basic stress-strain data at moderate strain rates (about 10^3 s^{-1}) are typically obtained in a Hopkinson-bar experiment in which an elastic wave is passed through a thin cylinder of the material under investigation. Strain gauges mounted on the support cylinders measure strain as a function of time. From these measurements, the stress-strain behavior of the material is inferred. The data from a Hopkinson-bar experiment on tantalum done at

room temperature (298°K) and a strain rate of 1300 s⁻¹ are shown in Fig. 1. This figure shows a well-known feature of Hopkinson-bar experiments, the presence of wiggles in the measured stress as a function of strain, which are particularly evident at strains of 0.02 and below but also observable at higher strains. These oscillations, caused by elastic wave dispersion within the sample and apparatus, tend to reduce the accuracy of Hopkinson-bar data. The data below strains of 0.017 seem unreliable because of their higher amplitude of the oscillations and the fact that the stress rises as the strain approaches zero instead of falling. Likewise, the data above a strain of 0.1 seem to be corrupted by an artifact. In the present analysis, the data in these two end regions are excluded.

To make use of the data between 0.017 and 0.1, their uncertainties need to be quantitatively characterized. The approach taken here is to treat the fluctuations in these data as a random Gaussian process with zero mean. The underlying assumption is that the measured signal fluctuates around its true value. The process is described as a random signal drawn from a Gaussian distribution with a covariance between two strains ϵ_i and ϵ_j given by $\sigma^2 \exp(-|\epsilon_i - \epsilon_j|^2/\lambda^2)$. The fluctuations are analyzed by first fitting a quadratic function to the data and subtracting it from them. The value of σ is the rms deviation of the resulting data set, which is found to be 4.9 MPa, or 0.8 %. By maximizing the likelihood function for the data, the correlation length λ is determined to be 0.0019. To avoid giving inappropriate weight to these data in the subsequent analysis, the measured data points are thinned by a factor equivalent to one sample per correlation length, which corresponds to using only every fourth measurement in this case. A similar analysis of the other Hopkinson-bar data sets yields σ values between 3.1 MPa and 5.3 MPa, and correlation lengths between 0.0027 to 0.0055.

The same type of analysis is carried out for the quasi-static measurements. However, these data do not exhibit the same oscillatory fluctuations around a smooth curve and the meaning of this kind of analysis is less clear. The rms deviation of the quasistatic data from a smooth second- or third-order curve is about 0.35 MPa, or only about 0.04% to 0.09%. Each of these data sets are also thinned out to around ten data points to avoid giving them undue influence in the following analysis.

Particularly for the quasi-static data, experience suggests caution in accepting the results of the above analysis without critical assessment. A number of assumptions are typically made about the physics in these experiments, which may well limit the overall accuracy of the reported data to a few percent. The actual uncertainties in these data are ultimately dominated by the systematic effects discussed below.

The above analysis leads to the final set of tantalum data shown in Fig. 2, in which the standard error in each datum is displayed as an error bar.

In addition to the suite of data shown in Fig. 2, an auxiliary set of four experiments were carried out at room temperature and 0.001 s⁻¹ strain rate to ascertain the degree of reproducibility from one tantalum sample to the next. The samples were selected from different lots with various processing histories to get a good idea of the amount of variability one might see in commercially obtained tantalum. With just four samples to go on, the rms deviation in measured stress values is about 8%. Note that this is a systematic error that is common to all the data from a single tantalum sample.

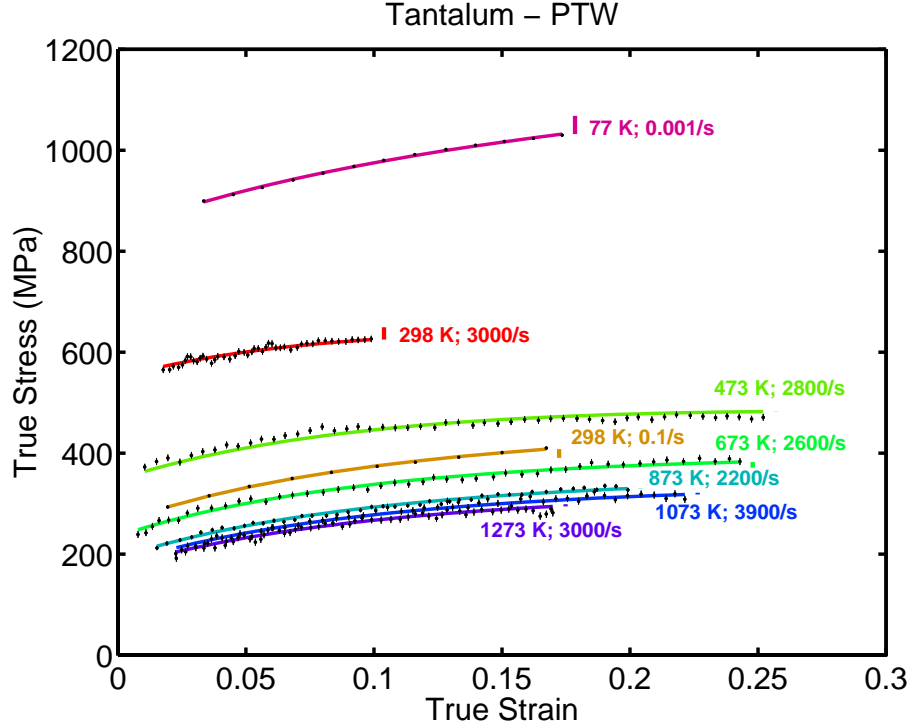


Figure 2. Comparison between data from material-characterization experiments for a variety of temperatures and strain rates and the PTW model fit to the data, shown as lines. The vertical bar to the right of each curve indicates the estimated systematic offset for that curve.

The tantalum specimens that yielded the data shown in Fig. 2 were obtained from a single lot so one would expect less sample-to-sample variation than in the above study. It seems reasonable to assign a systematic standard error of 3% to each of the displayed data sets. This assignment is supported by the degree of consistency between the data and the fitted model.

I include this sample-to-sample variability in the analysis by treating it as a systematic uncertainty. Because the observed differences between different samples amount to a small vertical shift of the curves, it is a good approximation to incorporate them in terms of an additive offset parameter for each curve. This effectively adds eight more parameters to the model, which need to be estimated as well as the parameters in the PTW model. To include this systematic effect in a full analysis of the eight data sets, the appropriate expression for the minus-log-likelihood is

$$-\log p(\mathbf{a} | \mathbf{d}) = \frac{1}{2} \sum_k \chi_k^2 + \frac{1}{2} \sum_k \frac{\Delta_k^2}{\sigma_k^2}, \quad (11)$$

where the index k identifies the data set obtained with a specific tantalum sample. The first term is a sum of χ^2 values for each data set at a specific temperature and strain rate. The second sum represents the prior probability for the offset parameters Δ_k , and σ_k is the rms deviation of the prior distribution on Δ_k , in the current analysis taken to be 3%

Table 1. PTW parameters for tantalum obtained from this preliminary analysis (fit4a) of the data shown in Fig. 2. All parameters are dimensionless.

Parameter	Value	Standard error
y_0	0.0123	0.0006
y_∞	0.00164	0.00004
s_0	0.0164	0.0007
s_∞	0.00308	0.00005
κ	0.91	0.08
γ	0.0000024	0.000002
θ	0.0145	0.0002

Table 2. Correlation coefficient matrix for the PTW model parameters obtained from the fit to the data shown in Fig. 2. The covariance matrix is estimated using Eqs. (4) and (6).

Parameter	y_0	y_∞	s_0	s_∞	κ	γ	θ
y_0	1	0.186	0.988	0.400	0.687	-0.464	-0.182
y_∞	0.186	1	0.208	0.913	0.142	0.022	-0.140
s_0	0.988	0.208	1	0.432	0.713	-0.496	-0.299
s_∞	0.400	0.913	0.432	1	0.443	-0.263	-0.257
κ	0.687	0.142	0.713	0.443	1	-0.935	-0.119
γ	-0.464	0.022	-0.496	-0.263	-0.935	1	0.087
θ	-0.182	-0.140	-0.299	-0.257	-0.119	0.087	1

of the mean stress value of the the k th data set. This term is needed to constrain the offset of the curves. Without it, the PTW parameters would be indeterminate.

The above model is fit to the data shown in Fig. 2 using the general approach described earlier to minimize the function given in Eq. (11). The Jacobian (sensitivity) matrix is estimated at each optimization iteration by the straightforward method of finite differences. In this fit, the following parameters are taken to be fixed: $G_0 = 654$ kilobars, $\alpha = 0.47$, $p = 4$, $A = 180.95$, $T_m = 3250^\circ\text{K}$, and $\rho = 16.6 \text{ g/cm}^3$. The value $p = 4$ is determined by auxiliary experiments that reach total strains of almost unity.[8] The following PTW parameters are not important because the strain rates are not high enough: y_1 , y_2 , and β . Adiabatic heating of the high strain-rate samples is taken into account, assuming a specific heat capacity of 0.15.

The fit to the data obtained in this preliminary analysis is shown in Fig. 2. The value of chi squared for 314 data points for this fit is 563, which corresponds to a chi squared per degree of freedom of approximately 1.9. The vertical bars to the right end of each curve

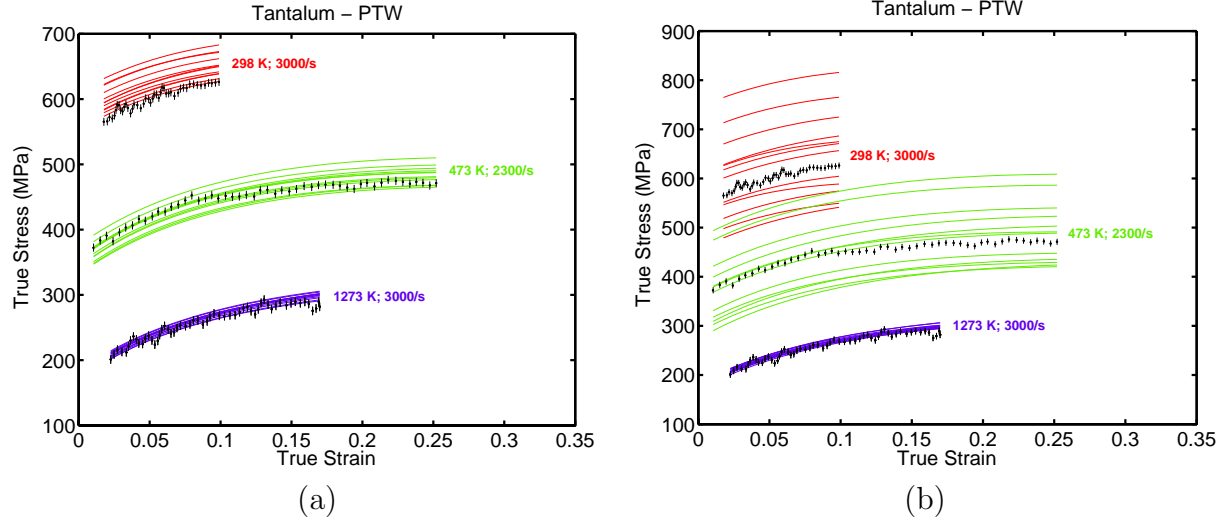


Figure 3. (a) A set of plausible stress-strain curves for three data sets (from top to bottom, 298°K, 1300 s⁻¹; 298°K, 0.1 s⁻¹; 1073°K, 3900 s⁻¹) obtained by drawing Monte Carlo samples from the uncertainty distribution in the PTW parameters as derived from the data shown in Fig. 2, and evaluating the PTW formulae. (b) Same as for (a), except that the correlations given in Table 2 are neglected. The ranges of variation for these curves are up to twice as larger as those observed in (a).

display the fitted value for the offset of that curve. The eight offset values range from -25 MPa to 14 MPa. The offsets contribution to chi-squared is 12.3 (the second term in Eq. 11), which is a reasonable value for eight parameters demonstrating consistency with their assumed rms deviation of 3%. The PTW parameters obtained from the fit and their rms uncertainties are given in Table 1. As important as the uncertainties in the individual parameters are, their correlation coefficients, presented in Table 2, are equally important. Use of the rms errors without consideration of the correlation coefficients would seriously misrepresent the results of this analysis, as will be demonstrated next.

The Monte Carlo technique described in Sect. 2 can be used to randomly draw PTW parameter vectors from their uncertainty distribution specified in Tables 1 and 2. Figure 3 shows a plot of the stress-strain curves that result from 12 such random draws for three data sets at different operating conditions. Because negative values of γ are not allowed in the PTW formalism and its relative error is so large, a log-normal distribution is used for that variable. From the comparison of these curves to the Hopkinson-bar measurements, one can conclude that the parameters and their uncertainties plausibly represent the data. However, the high value of chi squared mentioned above needs to be considered in a final analysis of these data. It indicates that either the uncertainties assigned to the data are too small or a discrepancy exists between the PTW model and the data. The Centroidal Voronoi Tessellation (CVT) [9, 10] algorithm is used here for drawing samples with more uniform spacing than a set of random samples would provide.

5. ANALYSIS OF TAYLOR DATA USING A SIMULATION CODE

The Taylor impact test represents an experiment of an intermediate level of complexity in the hierarchy of experiments chosen to elucidate the material model for tantalum. In the Taylor impact test, a cylindrical sample of material is propelled into a fixed, rigid surface. Taylor tests are often performed to confirm the plastic-behavior model of a material under severe strain conditions. Extremely high plastic strains and strain rates occur at the crushed end of the rod, resulting in severe local deformation [11, 12]. The experimental data usually consist of measurements of its final deformed profile.

The data from a Taylor experiment may be analyzed in much the same way as was done above for the material-characterization experiments. Systematic experimental uncertainties in the impact velocity, for example, may be included in a way similar to that used above to include the sample-to-sample variations. A contribution similar to the second term in Eq. (11) is necessary to account for the systematic offset for the specific sample used in the Taylor test. One viable approach to chi-squared minimization is to use the same methods as described above. When the simulation code is treated as a black box, the Jacobian matrix may be estimated by the method of finite differences. When the simulation code is available, however, the more sophisticated method of automatic differentiation may prove useful [13, 14].

Bayes theorem provides the proper means for combining the prior probability density function from the first analysis with the likelihood of the subsequent Taylor analysis [2]. The uncertainties from the above analysis may be included by adding to the expression given in Eq. (11) a term to represent the prior for the Taylor analysis, namely $\frac{1}{2}(\mathbf{a} - \hat{\mathbf{a}}_1)^T \mathbf{C}_1^{-1}(\mathbf{a} - \hat{\mathbf{a}}_1)$, where $\hat{\mathbf{a}}_1$ is the PTW parameter vector estimated in the foregoing analysis and \mathbf{C}_1 is the estimated covariance matrix.

When this process is employed to simply adjust the values of the model parameters to match the new data, it is called calibration, which is different from what I am proposing. By basing this parameter-updating process on Bayes theorem and quantitative uncertainty estimates, the process of Bayesian calibration becomes one of continuing inference [13]. In a sense, the Monte Carlo technique for estimating uncertainties in simulation-code output described above is reversed; the uncertainties in the parameters are determined from the combined uncertainties in the measurements and the effects on the simulation of uncertainties in experimental set up. Since the inference procedure involves determining the uncertainties in model parameters, it provides the means for predicting the uncertainty in simulation output in other physical scenarios. Further details of the process are presented in Ref. 2.

The focus here has been on the parameters in the Preston-Tonks-Wallace model. The Bayesian methodology can address other questions, for example, comparison of two or more competing models to decide between them. It is generally applicable to answering all questions that one might pose about models [15].

Acknowledgments

I gratefully acknowledge Shuh-Rong Chen's assistance, both by supplying the experimental data presented here and by providing considerable guidance in regard to material-

science issues. The following people have kindly shared their insights with me: Francois Hemez, Rusty Gray, Paul Maudlin, Larry Hull, Tom Duffey, Mark Anderson, Bill Oberkampf, Tim Trucano, Scott Doebling, C. Shane Reese, Dave Higdon, Mike McKay, and Kathy Campbell.

REFERENCES

1. K. M. Hanson and G. S. Cunningham. Validation of hydrocode predictions (U). In Edward Caramana and Charlie McMillan, editors, *Proc. 8th Nucl. Expl. Code Devel. Conf.*, pages 457–462. Report LA-12963-C, Los Alamos National Laboratory, 1995. (separately as Report LA-UR-01-6671).
2. K. M. Hanson. A framework for assessing uncertainties in simulation predictions. *Physica D*, 133:179–188, 1999.
3. K. M. Hanson and François M. Hemez. A framework for assessing confidence in computational predictions. *Exper. Techniques*, 25:50–55, 2001.
4. P. R. Bevington and D. K. Robinson. *Data Reduction and Error Analysis for the Physical Sciences*. McGraw-Hill, Boston, 1992.
5. G.H. Golub and C. F. Van Loan. *Matrix Computations*. Johns Hopkins Univ. Press, Baltimore, 1996.
6. Dean L. Preston, Davis L. Tonks, and Duane C. Wallace. Model of plastic deformation for extreme loading conditions. *J. Appl. Phys.*, 93:211–220, 2003.
7. Duane C. Wallace. Irreversible thermodynamics of overdriven shocks in solids. *Phys. Rev. B*, 24:5597–5606, 1981.
8. S. R. Chen, private communication. (2004).
9. Qiang Du, Vance Faber, and Max Gunzburger. Centroidal Voronoi Tessellations: Applications and algorithms. *SIAM Rev.*, 41:637–676, 1999.
10. Lili Ju, Qiang Du, and Max Gunzburger. Probabilistic methods for centroidal Voronoi tessellations and their parallel implementations. *Parallel Computing*, 28:1477–1500, 2002.
11. G. T. Gray III *et al.* Bridging the experimental-modeling gap - the Taylor test: an integrated test used to validate constitutive models. *to appear in AMPTIAC Newsletter*, 2002.
12. P. J. Maudlin *et al.* On the modeling of the Taylor cylinder impact test for orthotropic textured materials: experiments and simulations. *Int. J. Plasticity*, 15:139–166, 1999.
13. K. M. Hanson, G. S. Cunningham, and S. S. Saquib. Inversion based on computational simulations. In G. J. Erickson, J. T. Rychert, and C. R. Smith, editors, *Maximum Entropy and Bayesian Methods*, pages 121–135. Kluwer Academic, Dordrecht, 1998.
14. A. Griewank. *Evaluating Derivatives: Principles and Techniques of Automatic Differentiation*. SIAM, Philadelphia, 2000.
15. D. S. Sivia. *Data Analysis - A Bayesian Tutorial*. Clarendon, Oxford, 1996.